

Combined representation method for use in band-structure calculations: Application to highly compressed hydrogen*

Carlos Friedli[†] and N. W. Ashcroft

Laboratory of Atomic and Solid State Physics and Materials Science Center, Cornell University, Ithaca, New York 14853

(Received 19 January 1977)

A representation is described whose basis functions combine the important physical aspects of a finite set of plane waves with those of a set of Bloch tight-binding functions. The chosen combination has a particularly simple dependence on the wave vector \vec{k} within the Brillouin zone, and its use in reducing the standard one-electron band-structure problem to the usual secular equation has the advantage that the lattice sums involved in the calculation of the matrix elements are actually independent of \vec{k} . For systems with complicated crystal structures, for which the Korringa-Kohn-Rostoker, augmented-plane-wave, and orthogonalized-plane-wave methods are difficult to use, the present method leads to results with satisfactory accuracy and convergence. It is applied here to the case of compressed molecular hydrogen taken in a *Pa*3 (α -nitrogen) structure for various densities but with mean interproton distance held fixed. The bands show a marked free-electron character above 5 to 6 times the normal density, and the overall energy gap is found to vanish at 9.15 times normal density. Within the approximations made, this represents an upper bound for the molecular density in the transition to the metallic state from an α -nitrogen structure.

I. INTRODUCTION

The method described below evolved from an attempt to obtain the band structure of a system such as molecular hydrogen in a relatively complex crystal structure, and over a range of densities. For certain regions of the density it is expected on general grounds that neither the low-density tight-binding approach [with a representation of linear combinations-of-atomic-orbitals (LCAO) Bloch functions] nor the methods using a representation with a basis of simple plane waves (PW) are physically adequate.

For reasons principally connected with the structure, the other familiar methods are also not entirely adequate,^{1,2} at least in their standard formulations. The Korringa-Kohn-Rostoker (KKR) and augmented-plane-wave methods not only require a substantial amount of computational effort, but are based on a muffin-tin approximation to the actual one-electron potential.³⁻⁵ This means a "sphericalization" (taking the average over angles) of the potential arising from the contents of a unit cell, a procedure which is difficult to justify when the molecules in the crystal have no obvious spherical symmetry. Although such models yield useful physical information especially at lower densities, it is difficult to estimate their accuracy, particularly at higher densities, where steric effects and the requirements of proper crystal symmetry may become important. The effects of the latter on the resulting band structure may well be important as has been shown by Painter⁶ in his treatment of non-muffin-tin corrections to KKR bands by the discrete variational method.⁷

Furthermore, there is often no clear-cut sep-

aration between core levels (actually nonexistent for hydrogen) for which tight binding is adequate, and the rest of the band levels (valence and conduction), which would make an orthogonalized-plane-wave method appropriate. Even if one makes an arbitrary separation between valence and conduction levels, and treats the first with tight-binding functions and the second with orthogonalized-plane-wave functions orthogonalized to the valence levels,⁸ one still has the possibility of significant overlap of these "core" levels in situations such as the one here, where large variations in density are of physical interest.

For these reasons it is natural to investigate alternative representations whose basis functions combine in some way the advantages of both the LCAO functions (with their physically correct atomic behavior near the nuclei) and the PW, which are more satisfactory in the region between atoms. One such basis set was recently used by Ramaker *et al.*⁹ in exact-exchange crystal Hartree-Fock calculations of molecular and metallic hydrogen. Another, based on a more general and flexible approach, is described below. It is a modification of an idea used successfully by Brown and Krumhansl,¹⁰ which was shown to be mathematically equivalent to the orthogonalized-plane-wave method.

In Sec. II, the representation will be developed and its basic properties described. Section III is devoted to a discussion of the application of the representation to the solution of the one-electron problem in crystals. In Sec. IV, we present the results of the applications of the method to molecular hydrogen [assumed to be in α -nitrogen (*Pa*3) crystal structure] over a wide range of densities,

but with interproton distance generally held fixed. The most interesting point to emerge from the resulting band structure is the observation that valence and conduction bands begin to overlap at a lattice constant of $a = 4.78$ bohr, which corresponds to a density equal to 9.15 times its zero-pressure value. If the crystalline phase remains stable at such densities, this represents a metal-insulator transition at a density of approximately 0.83 g/cm^3 .

II. REPRESENTATION

The representation we introduce is formally incomplete: It has a finite set of basis wave functions. This set is made up of a finite number of PW and a set of specially constructed Bloch functions. It is constructed in such a way that the whole set is orthonormal, and although the set is finite, linear combinations of them are expected to give variationally good approximations to the eigenfunctions and corresponding eigenvalues. This expectation is based on the physical way the set is constructed, which will be explained in what follows.

Consider first a monatomic (for example, a simple cubic) lattice with lattice constant a and LCAO Bloch function $h_{\vec{k}}(\vec{r})$ defined with atomic orbital $\Phi(\vec{r})$,

$$h_{\vec{k}}(\vec{r}) = \frac{1}{\sqrt{N}} \sum_{\vec{R}} e^{i\vec{k}\cdot\vec{R}} \Phi(\vec{r} - \vec{R}), \quad (1)$$

where N is the number of cells in a volume Ω , \vec{R} designates their position vectors, and \vec{k} is the Bloch wave vector. Expressing this Bloch function in its well-known form

$$h_{\vec{k}}(\vec{r}) = \frac{1}{\sqrt{\Omega}} \sum_{\vec{K}} c_{\vec{k}-\vec{K}} e^{i(\vec{k}-\vec{K})\cdot\vec{r}}, \quad (2)$$

where \vec{K} is the set of reciprocal-lattice vectors corresponding to \vec{R} , it is easy to see that

$$c_{\vec{q}} = (N/\Omega)^{1/2} \Phi_{\vec{q}}^+, \quad (3)$$

where $\Phi_{\vec{q}}^+$ is the Fourier transform of $\Phi(\vec{r})$.

For the purposes of defining a trial function, $\Phi(\vec{r})$ may be *any* localized orbital, and not necessarily an atomic one. This observation will be used to construct a particularly convenient type of Bloch function. But instead of defining it directly (i.e., in \vec{r} space) it is inferred from conditions imposed on $c_{\vec{q}}^+$. In this way it is easier to enforce (through them) the properties that one would like the Bloch levels to have. First, some general observations:

One expects the eigenfunctions not to change too much very near (and particularly inside, if there is a core) the atoms or molecules forming the solid

from the values they assume in corresponding free atoms or molecules. This remains true even at fairly high densities. Thus, one wants to include in the basis set Bloch functions built with atomic or molecular orbitals to obtain a good representation in this region. But it is clear that for this purpose only those components $c_{\vec{k}-\vec{K}}$ with sufficiently large \vec{K} are relevant (here, \vec{k} is assumed to be restricted to the first Brillouin zone B_0). On the other hand, if the itinerant or free-electron character becomes important (as it will at high densities), plane waves with wave vectors (about the origin) not too large in terms of $2\pi/a$ are obviously indicated. We now construct basis functions incorporating these features. The Bloch function is first modified by truncating its Fourier components of low wave vectors, say \vec{G} , in some finite subset G of the reciprocal lattice K . In this way, the plane waves with wave vectors $\vec{k}-\vec{G}$ have been set free to be included in the basis set as independent members orthogonal to the Bloch functions. (For simplicity, in some of the algebraic manipulations the subset G may be chosen symmetrically to include both \vec{G} and $-\vec{G}$, although this is not required in general by the method.) For the simple-cubic-lattice case, for example, we may choose G to be the set of all reciprocal-lattice vectors within or on the surface of a cube centered at the origin, and with faces perpendicular to the axes. Further, let T be the complement of G , that is $G \cap T$ is empty and $G \cup T = K$. Next, the Bloch functions of the basis are to be chosen to have as *simple* a form as possible, a requirement for both analytical and computational purposes. In particular, the most simple functional dependence on \vec{k} is essential.

In the case of a Bravais lattice, a set of Bloch functions satisfying these criteria can be taken to have components

$$c_{\vec{q}} = \left(\frac{N}{\Omega}\right)^{1/2} \sum_{\vec{K}} \chi_{B_0}(\vec{q}-\vec{K}) \chi_T(\vec{K}) \Phi_{\vec{K}}, \quad (4)$$

where the characteristic function $\chi_A(\vec{x})$ is given by

$$\chi_A(\vec{x}) = \begin{cases} 1 & \text{if } \vec{x} \in A \\ 0 & \text{otherwise.} \end{cases}$$

Here, $\Phi(\vec{r})$ is a localized orbital. Figure 1 shows a schematic one-dimensional example of the procedure just outlined; there, the dotted curve represents the Fourier transforms $\Phi_{\vec{q}}$ of a localized orbital and the discontinuous curve the components $(\Omega/N)^{1/2} c_{\vec{q}}$ given by Eq. (4); note also that the set G contains *by choice* only the reciprocal-lattice vectors 0 and $\pm 2\pi/a$.

The functions defined by Eq. (4) all have the properties of Bloch functions, and can, of course, be written as

$$h_{\vec{q}}(\vec{r}) = \frac{1}{\sqrt{\Omega}} \sum_{\vec{k}} c_{\vec{q}-\vec{k}} e^{i(\vec{q}-\vec{k}) \cdot \vec{r}}. \quad (5)$$

This reduces, for $\vec{q} = \vec{k} \in B_0$, to the standard form

$$h_{\vec{k}}(\vec{r}) = e^{i\vec{k} \cdot \vec{r}} \left(\frac{\sqrt{N}}{\Omega} \sum_{\vec{k} \in T} \Phi_{\vec{k}} e^{i\vec{k} \cdot \vec{r}} \right), \quad (6a)$$

and is equivalent also to

$$h_{\vec{k}}(\vec{r}) = \frac{1}{\sqrt{N}} e^{i\vec{k} \cdot \vec{r}} \left[\sum_{\vec{R}} \Phi(\vec{r} - \vec{R}) - \frac{N}{\Omega} \sum_{\vec{G} \in G} \Phi_{\vec{G}} e^{i\vec{G} \cdot \vec{r}} \right]. \quad (6b)$$

where the quantity in square brackets clearly has the periodicity of the lattice. The prefactor in the expression for $c_{\vec{q}}$ is not important except to keep track formally, and in a consistent way, of the various constants and factors involved. (It cancels, of course, when normalizing the functions.)

The norm of $h_{\vec{k}}(\vec{r})$, $\|h\|$, is independent of \vec{k} and is given by

$$\|h\|^2 = \frac{N}{\Omega} \sum_{\vec{k} \in T} |\Phi_{\vec{k}}|^2, \quad (7)$$

or equivalently, by

$$\|h\|^2 = \sum_{\vec{R}} \langle \Phi(\vec{r}) | \Phi(\vec{r} - \vec{R}) \rangle - \frac{N}{\Omega} \sum_{\vec{G} \in G} |\Phi_{\vec{G}}|^2. \quad (8)$$

With the normalized functions $h_{\vec{k}}(\vec{r})/\|h\|$, the corresponding Wannier function $w(\vec{r})$ can be obtained,

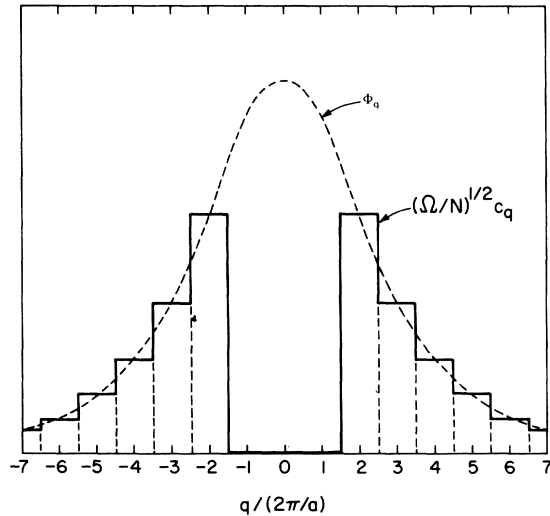


FIG. 1. Schematic one-dimensional example of components $(\Omega/N)^{1/2} c_q$ of a member of the new representation given by Eq. (4) (discontinuous curve) in terms of the Fourier transform Φ_q of a localized orbital (dotted curve). The reciprocal-lattice vectors correspond here to $q/(2\pi/a) = \text{integer}$. Note that c_q is identically zero in the central zones (corresponding to a choice here of a set of reciprocal-lattice vectors $G = \{-2\pi/a, 0, 2\pi/a\}$) and constant within each zone corresponding to the reciprocal-lattice vectors falling outside G (set T).

and is given by

$$w(\vec{r}) = \frac{1}{\|h\| \sqrt{N\Omega}} \sum_{\vec{q}}^{(\text{al1})} c_{\vec{q}} e^{i\vec{q} \cdot \vec{r}}, \quad (9)$$

which in this form is automatically normalized. It is, of course, orthogonal to $w(\vec{r} - \vec{R})$ for $\vec{R} \neq 0$. Substituting in Eq. (10) for $c_{\vec{q}}$, one gets

$$w(\vec{r}) = \frac{1}{\|h\|} \left(\frac{N}{\Omega} \right)^{1/2} \left(\sum_{\vec{k} \in T} \Phi_{\vec{k}} e^{i\vec{k} \cdot \vec{r}} \right) w_0(\vec{r}) \quad (10a)$$

or

$$w(\vec{r}) = \frac{1}{\|h\|} \left(\frac{\Omega}{N} \right)^{1/2} \left[\sum_{\vec{R}} \Phi(\vec{r} - \vec{R}) - \frac{N}{\Omega} \sum_{\vec{G} \in G} \Phi_{\vec{G}} e^{i\vec{G} \cdot \vec{r}} \right] w_0(\vec{r}), \quad (10b)$$

where for the case of a simple cubic Bravais lattice

$$w_0(\vec{r}) = \frac{1}{\sqrt{N\Omega}} \sum_{\vec{k} \in B_0} e^{i\vec{k} \cdot \vec{r}} = \left(\frac{N}{\Omega} \right)^{1/2} \frac{\sin(\pi x/a)}{\pi x/a} \frac{\sin(\pi y/a)}{\pi y/a} \frac{\sin(\pi z/a)}{\pi z/a} \quad (11)$$

is the empty lattice lowest-band Wannier function.

It is clear from the form of $h_{\vec{k}}(\vec{r})$ and $w(\vec{r})$ that these functions have the right behavior near and at the lattice sites \vec{R} , particularly if the finite set G does *not* contain large wave vectors. And for all $\vec{G} \in G$, $h_{\vec{k}}(\vec{r})$ is automatically orthogonal to the plane waves with wave vector $\vec{k} - \vec{G}$.

In this way, we have an incomplete but orthonormal basis set which would clearly be sufficient for a monatomic lattice if it were not necessary to use more than one localized $\Phi(\vec{r})$.

Except for small \vec{k} , the Bloch function $h_{\vec{k}}(\vec{r})$ just defined will *not* in general be a good approximation to the solution $\Psi_{\vec{k}}(\vec{r})$ of the one-electron problem of the crystal if G is empty (i.e., if no PW are included in the basis). The functions $h_{\vec{k}}(\vec{r})$ and $\Psi_{\vec{k}}(\vec{r})$ can differ substantially for larger \vec{k} , particularly near the boundaries of the Brillouin zone, simply because the Fourier components of $e^{-i\vec{k} \cdot \vec{r}} \Psi_{\vec{k}}(\vec{r})$ are functions of \vec{k} , while those of $e^{-i\vec{k} \cdot \vec{r}} h_{\vec{k}}(\vec{r})$ are not. Nevertheless, considering their expansions in reciprocal space, we find that as \vec{k} increases, the difference in their components *decrease*, since by *construction* both functions have the same form inside the atoms. Therefore, by truncating the components of low \vec{k} , and including the corresponding PW with wave-vector $\vec{k} - \vec{k}$ in the basis, we will increasingly improve the approximation as the number of PW increases.

Certainly it would be a better approximation to start by truncating the usual tight-binding Bloch

function $h_{\vec{k}}^{\text{TB}}(\vec{r})$ [defined with $\Phi(\vec{r})$] and choosing components

$$c_{\vec{q}} = (N/\Omega)^{1/2} \Phi_{\vec{q}}, \quad (12)$$

so that

$$h_{\vec{k}}^{\text{TB}}(\vec{r}) = \frac{\sqrt{N}}{\Omega} \sum_{\vec{k} \in \tau} \Phi_{\vec{k}-\vec{k}} e^{i(\vec{k}-\vec{k}) \cdot \vec{r}}. \quad (13)$$

However, this would not have the immense computational advantages of form (6), which permits all the terms there to be expressed in lattice sums *independent* of \vec{k} . Nevertheless, for some cases, higher accuracy requirements together with the necessity to keep the number of PW within reasonable limits might make it mandatory to use better Bloch functions than those defined by Eq. (6). {One way of defining these that would still give lattice sums independent of \vec{k} , is to take

$$c_{\vec{k}-\vec{k}} = (N/\Omega)^{1/2} [\Phi_{-\vec{k}+\vec{k}} \cdot (\nabla_{\vec{k}} \Phi_{\vec{k}-\vec{k}})_{\vec{k}=0} + \dots] \quad (14)$$

up to some order, but, of course, the higher the order chosen, the more cumbersome and time consuming become the computations.}

For the case where a set of more than one linearly-independent localized orbital must be used, a special Bloch function $h_{\vec{k}}(\vec{r})$ must be included for each. If the cell contains several atoms, say M atoms, with position vectors \vec{B}_i ($i=1, 2, \dots, M$), a set $h_{\vec{k}}(\vec{r} - \vec{B}_i)$ ($i=1, 2, \dots, M$) of linearly-independent Bloch functions, or M -independent linear combinations of them, must be included in the basis set. All the special Bloch functions are assumed constructed with a truncated set of plane waves of wave vectors $\vec{k} - \vec{G}$ with reciprocal-lattice vectors \vec{G} belonging to one and the same subset G . The basis will then contain for the same \vec{k} (other than the truncated set of plane waves) a set of linearly independent Bloch functions orthogonal to them but not in general to each other. An orthogonalization procedure must then be used to get an orthonormal basis set. The use of this orthonormal basis ultimately results in a secular equation with the energy eigenvalues residing *only* on the main diagonal, and has distinct analytical and computational advantages. The selection of one particular linearly independent set of Bloch functions (over other possible equivalent sets) depends on a judicious evaluation (as far as this possible) of how well they represent the true eigenfunctions of the crystal, and how their form may help the orthogonalization procedure in efficiently producing a physically convenient orthogonal set.

Let the initial set of Bloch functions, *before the orthogonalization procedure*, be a set of linearly independent combinations defined by

$$f_{n\vec{k}}(\vec{r}) = \sum_{j=1}^M a_{nj} h_{j\vec{k}}(\vec{r}), \quad n=1, 2, \dots, M \quad (15)$$

where the constants a_{nj} will be determined shortly. Here, the $h_{j\vec{k}}(\vec{r})$ are the Bloch functions defined for simplicity (but without loss of generality) with only one localized orbital in one of the monatomic sublattices of the basis. Hence,

$$h_{j\vec{k}}(\vec{r}) = h_{\vec{k}}(\vec{r} - \vec{B}_j). \quad (16)$$

Now we use the Gram-Schmidt orthogonalization procedure to get from $\{f_{n\vec{k}}\}$ an orthogonal set $\{g_{n\vec{k}}\}$. The $g_{n\vec{k}}$ have the following recursion relations:

$$|g_{1\vec{k}}\rangle = |f_{1\vec{k}}\rangle, \quad (17)$$

$$|g_{n\vec{k}}\rangle = \frac{|f_{n\vec{k}}\rangle}{\|f_{n\vec{k}}\|} - \sum_{m=0}^{n-1} \frac{|g_{m\vec{k}}\rangle}{\|g_{m\vec{k}}\|} \frac{\langle g_{m\vec{k}} | f_{n\vec{k}} \rangle}{\|f_{n\vec{k}}\|}$$

for $n=2, 3, \dots, M$,

and the norms $\|g_{n\vec{k}}\|$ are given by

$$\|g_{n\vec{k}}\|^2 = 1 - \sum_{m=0}^{n-1} \frac{|\langle g_{m\vec{k}} | f_{n\vec{k}} \rangle|^2}{\|g_{m\vec{k}}\|^2 \|f_{n\vec{k}}\|^2}. \quad (18)$$

These may be used in slightly modified form which subsequently reduces the numerical work. Let $g_{n\vec{k}}(\vec{r})$ be expressed first as linear combinations of $h_{j\vec{k}}(\vec{r})$:

$$|g_{n\vec{k}}\rangle = \sum_j b_{nj\vec{k}} |h_{j\vec{k}}\rangle \quad \text{for } n=2, 3, \dots, M. \quad (19)$$

Then,

$$\langle g_{m\vec{k}} | f_{n\vec{k}} \rangle = \sum_i \sum_j b_{mi\vec{k}}^* a_{nj} \langle h_{i\vec{k}} | h_{j\vec{k}} \rangle, \quad (20)$$

and

$$b_{nj\vec{k}} = \frac{a_{nj}}{\|f_{n\vec{k}}\|} - \sum_{m=0}^{n-1} b_{mj\vec{k}} \frac{\langle g_{m\vec{k}} | f_{n\vec{k}} \rangle}{\|g_{m\vec{k}}\|^2 \|f_{n\vec{k}}\|} \quad \text{for } n=2, 3, \dots, M. \quad (21)$$

(Note that, in general, these are functions of \vec{k} .)

Further,

$$\|f_{n\vec{k}}\|^2 = \sum_i \sum_j a_{ni}^* a_{nj} \langle h_{i\vec{k}} | h_{j\vec{k}} \rangle. \quad (22)$$

Next, let an orthonormal (incomplete) basis set $\{\Psi_{\alpha\vec{k}}^{(0)}(\vec{r}), \alpha \in A, \vec{k} \in B_0\}$ be defined by

$$\Psi_{\alpha\vec{k}}^{(0)}(\vec{r}) = \begin{cases} \Psi_{\vec{G}\vec{k}}^{(0)}(\vec{r}) = (1/\sqrt{\Omega}) e^{i(\vec{k}-\vec{G}) \cdot \vec{r}} & \text{for } \alpha = \vec{G} \in G, \\ \Psi_{n\vec{k}}^{(0)}(\vec{r}) = g_{n\vec{k}}(\vec{r}) / \|g_{n\vec{k}}\| & \text{for } \alpha = n, 1 \leq n \leq M. \end{cases} \quad (23)$$

Then, $A = G \cup \{n, 1 \leq n \leq M\}$. The superscript zero indicates this is a basis *in which to expand the unknown variational approximations to the eigenfunctions* $\Psi_{\vec{k}}(\vec{r})$, i.e.,

$$\Psi_{\vec{k}}(\vec{r}) = \sum_{\alpha \in A} x_{\alpha\vec{k}} \Psi_{\alpha\vec{k}}^{(0)}(\vec{r}). \quad (24)$$

Equation (24), as an expansion of the one-electron function, will be used in Sec. III as a trial function for the one-electron problem in crystals. Note that, although incomplete, the finite basis set (23) is orthonormal and contains by construction localized orbitals appropriate for the cores of the molecules forming the crystal and plane waves adequate for the *intermolecular* region. Therefore, we can expect linear combinations of them to be good approximations for the eigenfunctions of the lower bands, the accuracy improving as the number of PW in G increases, particularly for \vec{k} near the boundaries of the Brillouin zone.

III. APPLICATION TO THE SOLUTION OF THE ONE-ELECTRON PROBLEM IN CRYSTALS

Substituting Eq. (24) into the one-particle Schrödinger equation for the crystal, the band-structure problem reduces to

$$\sum_{\beta \in A} H_{\alpha\beta\vec{k}} x_{\beta\vec{k}} = E_{\vec{k}} x_{\alpha\vec{k}} \quad \text{for all } \alpha \in A, \quad (25)$$

with

$$H_{\alpha\beta\vec{k}} = \langle \Psi_{\alpha\vec{k}}^{(0)} | \hat{H} | \Psi_{\beta\vec{k}}^{(0)} \rangle. \quad (26)$$

Here, \hat{H} is the single-particle crystal Hamiltonian. The reason why only one \vec{k} is involved everywhere is the usual one, that \hat{H} is a linear operator invariant under the translation group of the crystal, for which

$$\langle \Psi_{\alpha\vec{k}}^{(0)} | \hat{H} | \Psi_{\beta\vec{k}}^{(0)} \rangle = \delta_{\vec{k}\vec{k}'} \langle \Psi_{\alpha\vec{k}}^{(0)} | \hat{H} | \Psi_{\beta\vec{k}}^{(0)} \rangle. \quad (27)$$

The matrix elements $H_{\alpha\beta\vec{k}}$ are given by

$$H_{\vec{G}\vec{G}\vec{k}} = (\hbar^2/2m)(k - G)^2 \delta_{\vec{G}\vec{G}'} + U_{\vec{G}' - \vec{G}}, \quad (28)$$

$$H_{\vec{G}\vec{n}\vec{k}} = \sum_j b_{nj\vec{k}} \langle \Psi_{\vec{G}\vec{k}}^{(0)} | \hat{H} | h_j\vec{k} \rangle \|g_{n\vec{k}}\|^{-1} \quad (29)$$

$$H_{n'n\vec{k}} = \sum_i \sum_j b_{n'i\vec{k}}^* b_{ni\vec{k}} \langle h_j\vec{k} | \hat{H} | h_i\vec{k} \rangle \|g_{n'\vec{k}}\|^{-1} \|g_{n\vec{k}}\|^{-1}, \quad (30)$$

where the plane-wave matrix element of the local one-electron crystal potential is given by

$$U_{\vec{k}} = (N/\Omega) V_{\vec{k}}, \quad (31)$$

with

$$V_{\vec{k}} = \int d\vec{r} e^{-i\vec{k}\cdot\vec{r}} V(\vec{r}) \quad (32)$$

and

$$U(\vec{r}) = \sum_{\vec{R}} V(\vec{r} - \vec{R}). \quad (33)$$

Because of the special form [Eq. (6)] of $h_{i\vec{k}}(\vec{r})$, the products $\langle h_{i\vec{k}} | h_j\vec{k} \rangle$ and the matrix elements $\langle \Psi_{\vec{G}\vec{k}}^{(0)} | \hat{H} | h_j\vec{k} \rangle$ and $\langle h_{i\vec{k}} | \hat{H} | h_j\vec{k} \rangle$ can be expressed in terms of reciprocal (or reciprocal *and* direct) lat-

tice sums which are independent of the point in the Brillouin zone (all the \vec{k} dependence being factored out). For the case of only one localized orbital but with a basis of several atoms, we have

$$\langle h_{i\vec{k}} | h_j\vec{k} \rangle = (N/\Omega) e^{i\vec{k}\cdot(\vec{B}_i - \vec{B}_j)} S_{ij}, \quad (34)$$

$$\langle \Psi_{\vec{G}\vec{k}}^{(0)} | \hat{H} | h_j\vec{k} \rangle = (N/\Omega)^{1/2} e^{-i\vec{k}\cdot\vec{B}_j} S_{\vec{G}j}, \quad (35)$$

and

$$\langle h_{i\vec{k}} | \hat{H} | h_j\vec{k} \rangle = (N/\Omega) e^{i\vec{k}\cdot(\vec{B}_i - \vec{B}_j)} \times [(\hbar^2/2m)(S'_{ij} - 2i\vec{k}\cdot\vec{S}'_{ij} + k^2 S_{ij}) + S_{ij}^D], \quad (36)$$

where

$$S_{ij} = \sum_{\vec{k} \in \mathcal{T}} |\Phi_{\vec{k}}|^2 e^{i\vec{k}\cdot(\vec{B}_i - \vec{B}_j)}, \quad (37)$$

$$\vec{S}'_{ij} = \sum_{\vec{k} \in \mathcal{T}} i\vec{k} |\Phi_{\vec{k}}|^2 e^{i\vec{k}\cdot(\vec{B}_i - \vec{B}_j)}, \quad (38)$$

$$S''_{ij} = \sum_{\vec{k} \in \mathcal{T}} K^2 |\Phi_{\vec{k}}|^2 e^{i\vec{k}\cdot(\vec{B}_i - \vec{B}_j)}, \quad (39)$$

$$S_{\vec{G}j} = \sum_{\vec{k} \in \mathcal{T}} \Phi_{-\vec{k}} U_{\vec{G}-\vec{k}} e^{i\vec{k}\cdot\vec{B}_j}, \quad (40)$$

and

$$S_{ij}^D = \sum_{\vec{k} \in \mathcal{T}} \sum_{\vec{k}' \in \mathcal{T}} \Phi_{\vec{k}}^* \Phi_{\vec{k}'} U_{\vec{k}' - \vec{k}} e^{i(\vec{k}'\cdot\vec{B}_i - \vec{k}\cdot\vec{B}_j)}. \quad (41)$$

These lattice sums can be expressed in part as *direct* lattice sums, using the convolution theorem or by application of Eq. (6b). For example,

$$S_{ij} = \sum_{\vec{R}} \langle \Phi(\vec{r}) | \Phi(\vec{r} + \vec{B}_i - \vec{B}_j - \vec{R}) \rangle - \frac{N}{\Omega} \sum_{\vec{G} \in \mathcal{G}} |\Phi_{\vec{G}}|^2 e^{i\vec{G}\cdot(\vec{B}_i - \vec{B}_j)} \quad (42)$$

From this, \vec{S}'_{ij} and S''_{ij} can be obtained, respectively, by taking the gradient and the negative of the Laplacian with respect to the spatial variable. A similar result can be obtained with $S_{\vec{G}j}$ and S_{ij}^D , but here it would be of no advantage if only the Fourier transform of the potential is available.

The number of different lattice sums that must be actually computed is greatly reduced by exploiting crystal symmetries. First of all, the sums are invariant under a transposition of indices, except for \vec{S}'_{ij} (which only changes sign) and $S_{\vec{G}j}$. In general a simultaneous change of \vec{B}_i , \vec{B}_j , and \vec{G} (in the case of $S_{\vec{G}j}$) under the same cubic or other symmetry will also leave S_{ij} , S''_{ij} , $S_{\vec{G}j}$, and S_{ij}^D unaltered, and will take \vec{S}'_{ij} into the corresponding symmetric vector. In this way, for example, the 64 S_{ij}^D sums of the $Pa3$ (or α - N_2) crystal structure⁸ are reduced to only four, and the $S_{\vec{G}j}$ sums to only two for each \vec{G} , and in both classes of sums this leads to an enormous reduction in computational time.

Once the lattice sums are evaluated, we can proceed to solve the secular eigenvalue problem [Eq. (25)] for a particular \vec{k} by first obtaining the corresponding basis set [Eq. (23)] with the help of Eqs. (19)–(22), then the matrix elements $H_{\alpha\beta\vec{k}}$ with Eqs. (28)–(30), and finally diagonalizing Eq. (25). In this way, we obtain the valence and lowest conduction bands and the coefficients $\chi_{\alpha\vec{k}}$ in the expansion of the corresponding eigenfunctions in terms of the basis set [Eq. (23)].

IV. BANDS OF COMPRESSED MOLECULAR HYDROGEN

We turn now to an application of the combined-representations method to the case of solid H_2 in the α -nitrogen phase. It should be mentioned that this structure is not the only candidate for the ground-state configuration of molecular hydrogen.^{11–14} We have selected it here because of the various possibilities, it is lowest in symmetry and therefore represents the most complex case numerically. Other structures have higher symmetry and the method is computationally easier to apply.

The α - N_2 structure¹⁵ has the space group $Pa\bar{3}$. It is simple cubic with a basis of four molecules. In the case of hydrogen, there are eight protons and eight electrons per primitive cell. There are sufficient electrons to fill four valence bands provided there is no overlap with conduction bands. In most of the results discussed below, it is important to note that the interproton distance (0.741 Å) is held fixed at all densities considered. We return to this point in Sec. V.

To apply (25), we need to specify the one-electron potential $U(\vec{r})$ that best represents the interaction of the electrons with the protons and with themselves. Since we are mostly interested in the high-density situation we have taken this to result from the bare Coulomb interaction of the protons and screened by a Lindhard-type dielectric function. Unlike other systems, hydrogen has the advantage that the bare interactions are known precisely. The dielectric approach accounts for the bulk of the many particle effects and all residual uncertainty in $U(\vec{r})$ a reflection of exchange and correlation in the choice of the dielectric function itself. For the smallest reciprocal lattice vector that enters in (28), the dielectric function is already close to unity and such corrections are of diminishing concern as the density increases into the primary range of interest ($r_s \approx 1.5$).

The bands have been calculated along the standard simple cubic directions^{15,16} ΓX , MR , and $R\Gamma$ (see Fig. 2) for lattice constants of 10, 6, 5, and 4.5 bohrs. (Computational and other details may be found in the Appendix). These bands are shown

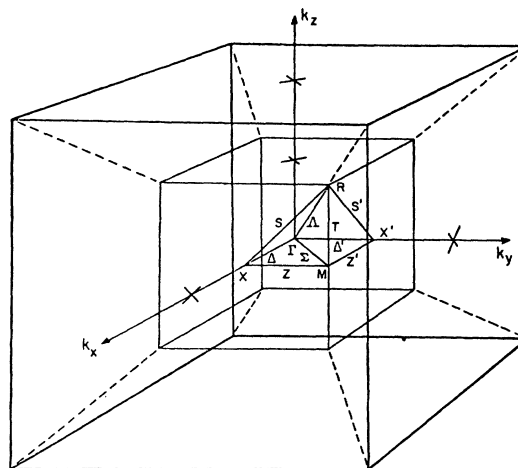


FIG. 2. The inner cube here is the Brillouin zone of the $Pa\bar{3}$ (α - N_2) crystal structure. The letters correspond to high-symmetry points and lines in the basic domain (unprimed) or the larger representation domain (including primes). The outer cube is limited by (100) planes, and is an example of a set G with $l_1=1$, containing, then, 27 reciprocal-lattice vectors.

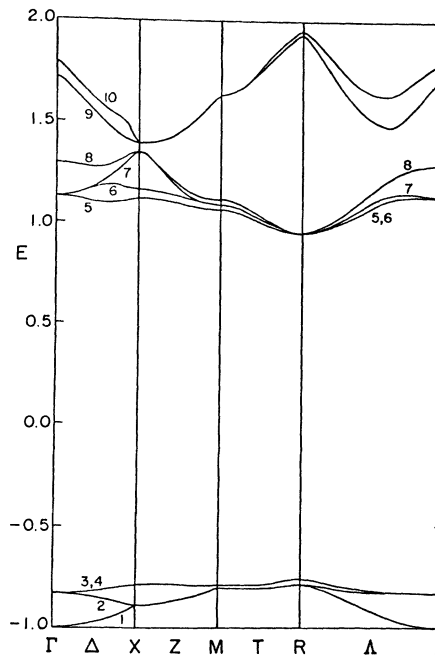


FIG. 3. Band structure of the α - N_2 phase of hydrogen, with lattice constant $a=10$ bohrs or equivalently, $r_s = 3.102$ (pressure zero). The energy E is normalized to $(\hbar^2/2m)(2\pi/a)^2 = 0.3948$ Ry. The numbers indicate, in order, the ten lowest bands calculated. Note that in order to display the overall form of the band structure the scale does not permit the resolution of certain bands. For example, in Figs. 4, 5, and 6, bands 2, 3, and 4 along $R\Gamma$ are not all degenerate as can be seen from Table I and also from this figure.

in Figs. 3–6. Figure 7 displays the empty lattice bands to which the bands at lattice constants 4.5, 5, and even 6 bohrs reveal a striking similarity. This nearly-free-electron character (at high density) gives at least *ex post facto* support to the dielectric formulation used in constructing the matrix elements of the potential.

Although the primary interest here is in the bands of highly compressed hydrogen it is worth noting that for the zero-pressure case ($a \sim 10$ bohr) we find an overall band gap of 9.2 eV. This is close to the observed value for the onset of absorption in the optical spectrum¹⁷; it is also close to the value deduced from energy-loss experiments.¹⁸ (Regarding the optical data, it must be said that there is, at present, disagreement in the interpretation of the data.^{19,20}) Further, the overall gap agrees well with the value of 10.7 eV obtained by Zunger²⁰ using a truncated crystal approach, and also with the energy of the lowest-allowed optical transition obtained by the KKR method.¹

V. RESULTS AND CONCLUSIONS

We first comment on the form of the bands of highly compressed hydrogen, and then on the method used to obtain these bands.

Referring to Figs. 4–6, perhaps the most inter-

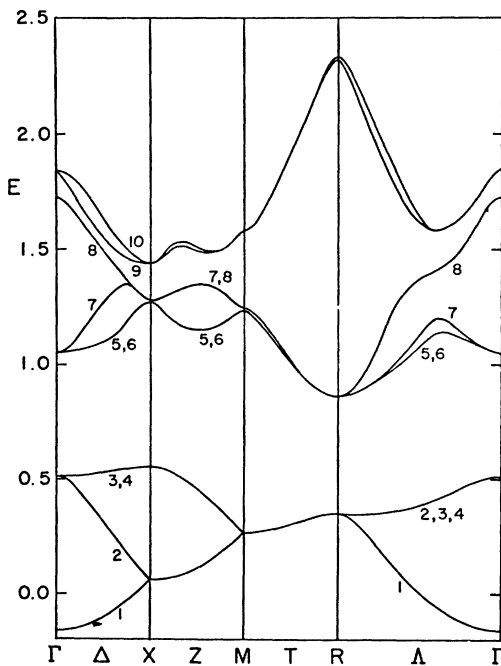


FIG. 4. Band structure of the α -N₂ phase of hydrogen with lattice constant $a=6$ bohrs or equivalently, $r_s=1.861$. The energy E is normalized to $(\hbar^2/2m)(2\pi/a)^2=1.0966$ Ry. The numbers indicate in order the ten lowest bands calculated.

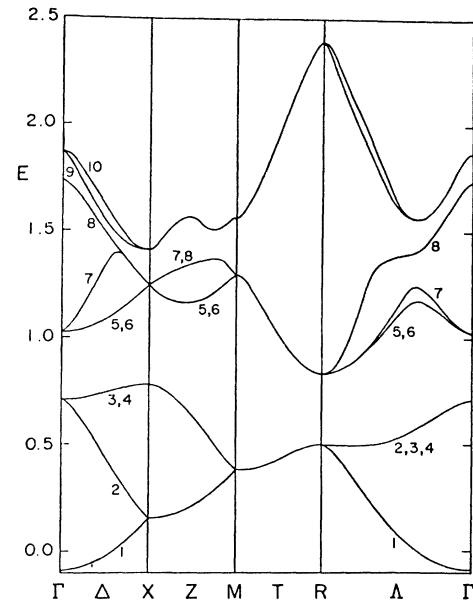


FIG. 5. Band structure of the α -N₂ phase of hydrogen, with lattice constant $a=5$ bohrs or equivalently, $r_s=1.551$. The energy E is normalized to $(\hbar^2/2m)(2\pi/a)^2=1.5791$ Ry. The numbers indicate in order the ten lowest bands calculated.

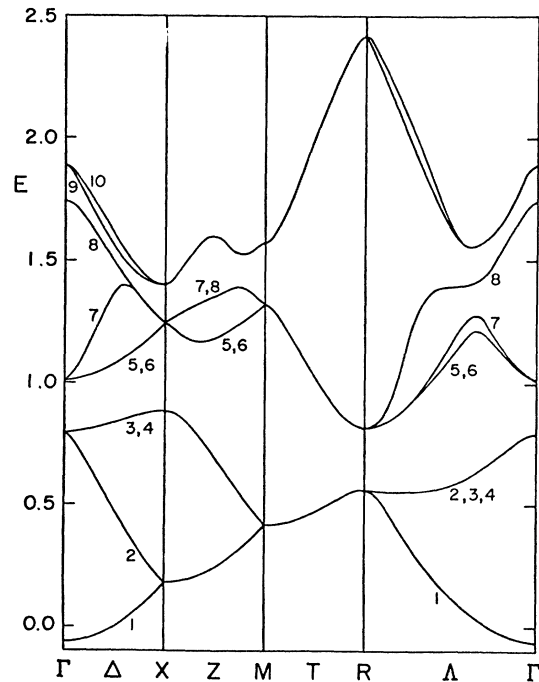


FIG. 6. Band structure of the α -N₂ phase of hydrogen, with lattice constant $a=4.5$ bohrs or equivalently, $r_s=1.396$. The energy E is normalized to $(\hbar^2/2m)(2\pi/a)^2=1.9496$ Ry. The numbers indicate in order the ten lowest bands calculated. Note that the overall band gap in Figs. 3–5 is no longer present in this figure.

esting point to emerge is the fact that the overall band gap (which becomes indirect at higher densities) vanishes at a lattice constant of $a = 4.78$ bohrs. The vanishing corresponds to the crossing of the highest valence band at X and lowest conduction band at R . In Fig. 8, this gap has been plotted [normalized to $(\hbar^2/2m)(2\pi/a)^2$] as a function of the lattice constant a , and the critical value $a = 4.78$ is determined by linear interpolation between the gap values for $a = 4.5$ and $a = 5$ bohrs. As suggested by the calculated points, the normalized gap varies almost linearly with a . For constant interproton distance, the vanishing of the gap represents a second-order metal-insulator transition, provided, of course, that the crystalline phase of metallic hydrogen remains stable up to this point in density. The point where the molecular phase becomes metallic, i.e., $\rho = 0.83 \text{ g/cm}^3$, represents a possible upper bound for the molecular density at which, for fixed interproton distance, the transition is made to a metallic state. The situation here therefore parallels somewhat the case of solid iodine in its progression with increasing pressure. As discussed recently by McMahan *et al.*²¹ the metallization of iodine is evidently not

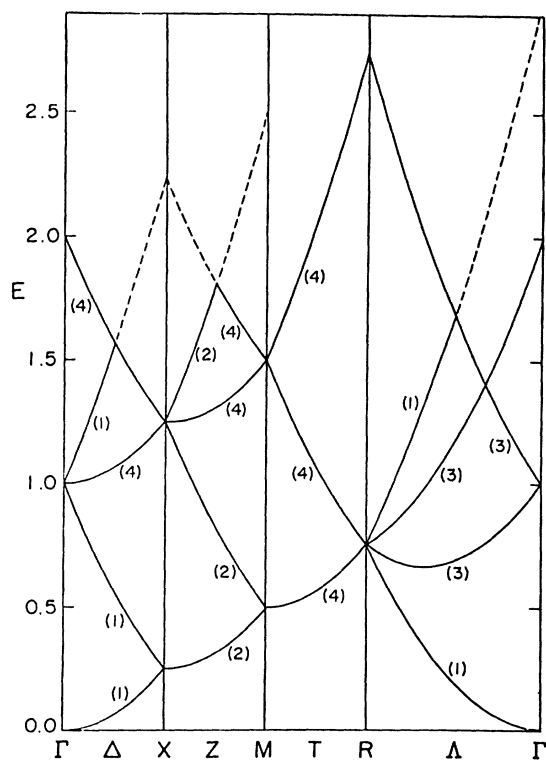


FIG. 7. Band structure of the sc empty lattice. The energy E is normalized to $(\hbar^2/2m)(2\pi/a)^2$. The numbers indicate the degeneracy of each band. The bands drawn with a full line are the limit to which the ten lowest calculated for H_2 tend as lattice constant approaches zero.

a first-order transition, at least at lower pressures, and a band-overlap phenomenon preceding total pressure dissociation is therefore possible.

It is important to reemphasize that the results just described are apposite to an approximation in which the protons are both static and held at constant interproton separation within molecules. The inclusion of lattice-dynamical effects, particularly at high density, can be expected to lead to noticeable corrections, as they do for crystalline phases of metallic hydrogen.^{22,23} As a decreases, we may expect the intermolecular electron density to increase in value at the expense of the intramolecular density. From a consideration of electrostatic terms alone, we would anticipate that expressed as a fraction of lattice constant, the interproton separation will increase with increasing density. A total energy calculation of the ground-state energy of molecular hydrogen will be required to determine this trend. However, a guide to the size of the effects associated with possible variations in interproton spacing $2D$ is relatively straightforward to obtain, since $2D$ is one of the basic input parameters. We have recomputed the bands of Figs. 5-7 with interproton spacing ranging between about 1.1 and 1.7 bohrs and from these have extracted by interpolation the density, for a given D , at which band overlap begins. The results are summarized in Fig. 9 as a line separating metallic from insulating regions for the $Pa3$ structure. The implication of the apparent linear trend over the limited range of parameters is that once a given band-overlap state has been attained, the interproton spacing is required to fall with unreasonable rapidity if such a state were imagined to pass once again into an insulating phase by imposing an additional increase in density.

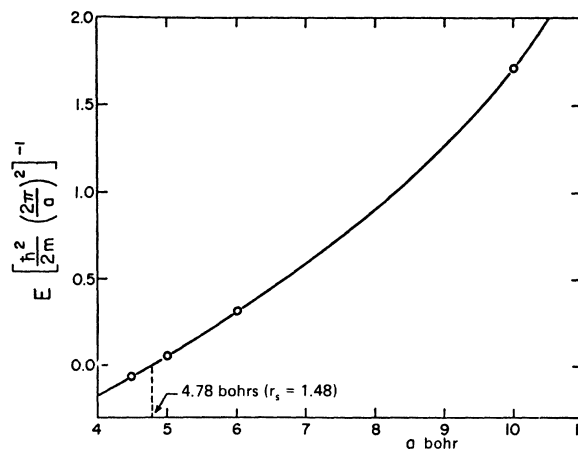


FIG. 8. Energy gap normalized to $(\hbar^2/2m)(2\pi/a)^2$ as a function of the lattice constant a . The solid line is an approximate interpolation between the calculated values, which are indicated by circles.

Finally, returning to the method itself, we have shown that the subspace spanned by the orthogonal finite basis set of functions [Eq. (23)] can be expected to yield a satisfactory approximation to the one-electron eigenfunctions for electrons moving in a periodic potential. The set is of manageable size and at the same time leads to good convergence by virtue of its construction in terms of orbitals which represent both intra- and inter-molecular features. This is accomplished in a rather simple way with a few plane waves and orbitals depending on \vec{k} only through a factor $e^{i\vec{k}\cdot\vec{r}}$. It leads, however, to lattice sums independent of \vec{k} when calculating the matrix elements of the secular problem [Eq. (25)], to which the band-structure problem has been reduced. As a consequence, it is necessary to evaluate the sums *only once* for a given lattice parameter and crystal structure. Even for low-symmetry structures, such as the one treated here, it is quite straightforward to obtain the necessary matrix elements in (25) for any \vec{k} in the zone.

The method does not require the muffin-tin approximation to the potential, as do the standard formulations of the KKR or augmented-plane-wave methods. It is readily adaptable to systems where non-muffin-tin corrections are likely to be important, such as molecular systems or systems with

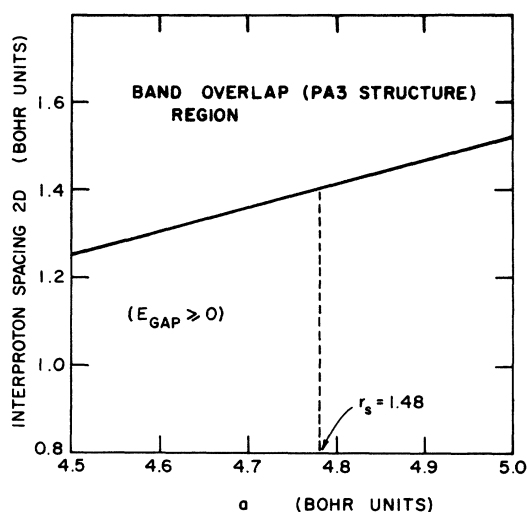


FIG. 9. A plot of the variation of interproton spacing $2D$ required, for a given density (or lattice spacing a) to lead to a vanishing of the overall band gap of H_2 in the $Pa3$ structure. The region above the line represents a ground-state metallic phase, below it the phase is insulating. Plotted vertically at $a=4.78$ is a line which intersects the boundary at an interproton spacing 1.4 bohrs. This summarizes the band-overlap results of Fig. 4-7. (Note that for a fixed lattice constant a reduction in $2D$ tends to lead in this range of densities to a stronger one-electron potential and hence to larger band gaps.)

complex crystal structures which can be treated, for example, by systematic correction of the KKR bands.⁶ The level of analytic complexity and computational difficulty does not exceed that of such methods. When compared specifically with the OPW method, its main advantage appears to be a simpler formulation which makes no specific reference to core levels.

TABLE I. Four valence bands and the lowest conduction band at selected points of the Brillouin zone and functions of l_1 and l_2 (see Appendix). Here, the lattice constant is $a=5$ bohrs, and energies are normalized to $(\hbar^2/2m)(2\pi/a)^2=1.5791$ Ry.

l_1	l_2	Γ	X	R
-1	4	1.3178	1.5679	2.4526
		0.7384	0.9659	1.1035
		0.7384	0.9519	1.1034
		0.7384	0.5479	0.8786
		-0.0537	0.1961	0.6948
-1	5	1.2930	1.5432	2.4314
		0.7261	0.9530	1.0875
		0.7261	0.9388	1.0875
		0.7260	0.5317	0.8619
		-0.0548	0.1951	0.6936
0	3	1.3739	1.5949	2.5006
		0.7655	0.9942	1.1387
		0.7655	0.9805	1.1386
		0.7655	0.5836	0.9032
		-0.0755	0.1737	0.6679
0	4	1.3176	1.5374	2.4526
		0.7384	0.9659	1.1034
		0.7384	0.9518	1.1033
		0.7384	0.5478	0.8668
		-0.0834	0.1656	0.6580
0	5	1.2927	1.5119	2.4275
		0.7260	0.9529	1.0874
		0.7260	0.9387	1.0873
		0.7260	0.5316	0.8505
		-0.0873	0.1616	0.6529
1	4	1.0318	1.2622	0.8442
		0.7347	0.8121	0.5407
		0.7247	0.8110	0.5407
		0.7247	0.1681	0.5381
		-0.0834	0.1592	0.5323
1	5	1.0283	1.2580	0.8428
		0.7146	0.8010	0.5344
		0.7146	0.8000	0.5344
		0.7146	0.1632	0.5318
		-0.0874	0.1549	0.5256
2	5	1.0246	1.2483	0.8318
		0.7111	0.7803	0.4994
		0.7111	0.7802	0.4990
		0.7111	0.1529	0.4990
		-0.0876	0.1504	0.4986

APPENDIX

In the calculation of the bands shown in Figs. 3-6, some parts of the lattice sums defined in Eqs. (37)-(41) were calculated in direct space and some in reciprocal space. In general, the choice is dictated by the convergence properties of the functions under consideration. For the present case, $\Phi(r)$ can be taken as a 1s orbital

$$\Phi(r) = (\alpha^3/\pi)^{1/2} e^{-\alpha r} \quad (\text{A1})$$

with Fourier transform

$$\Phi_{\vec{q}} = (\alpha^3/\pi)^{1/2} 8\pi\alpha / (q^2 + \alpha^2)^2.$$

The direct lattice sum in Eq. (42) requires²⁴

$$\langle \Phi(\vec{r} - \vec{r}') | \Phi(\vec{r}') \rangle = e^{-\alpha r} (1 + \alpha r + \frac{1}{3}\alpha^2 r^2),$$

which leads to rapid convergence in direct space for the s_{ij} , S'_{ij} , and S''_{ij} . Since S_{Gi} and S'_{ij} involve both $\Phi(r)$ (falling exponentially with r) and $V(r)$ (falling roughly as r^{-1}), a similar conclusion can be drawn about their convergence in direct space. But we also observe that in reciprocal space the convergence of the sums in (37)-(41) is also rapid since Φ_K falls as K^{-4} and U_K eventually as K^{-2} .

We turn now to general convergence properties. For the simple cubic system, we select G , on the basis of symmetry, to be all the reciprocal-lattice vectors within or on the surface of a cube centered on the origin, with faces perpendicular to the ones and aside of length $(2\pi/a)2l_1$ (see Fig. 2). Here, l_1 is a positive integer. Lattice sums in reciprocal space were computed by including only those terms with reciprocal-lattice vectors within and on the surface of a cube also centered at the origin and also having its faces normal to the axes. The side of this cube is taken as $(2\pi/a)(2l_2 + 1)$. [For sums in direct space, we include terms with di-

rect lattice vectors \vec{R} lying within and on the surface of a cube of side $(2l_R + 1)a$]. With these definitions the number N_{PW}^1 of plane waves in the basis set is $(2l_1 + 1)^3$: The corresponding number N_{PW}^2 of plane waves in the expansions of the ortho-normal Bloch functions of the basis is $(2l_2 + 1)^3 - N_{\text{PW}}^1$ (provided $l_2 > l_1$). Table I shows convergence of four valence-bands and the lowest conduction-band energies at selected points of the zone lattice constant $a = 5$ bohrs. (Note that the absence of any plane waves in the expansion is symbolically designated here by the choice $l_1 = -1$.) At these densities sums computed in direct space were found to converge for l_R below 4 or 5. Finally, the maximum matrix order used was 133; symmetries could be used to further reduce this number.

In constructing the Bloch functions for hydrogen, only a simple 1s orbital was used. That this is reasonable is indicated by the following: Let G contain reciprocal-lattice vectors with components of magnitude $\leq 2\pi/D$, where $2D$ is the interproton distance (about $1.4a_0$ if the separation is not much affected by pressure). With this range of reciprocal-lattice vectors, the truncated set of plane waves will then represent well the electron distribution in the intermolecular region. The inclusion of 1s orbitals will give a good representation within the molecule for spatial variations in the wave function no more rapid than a change of sign in going from one proton in a molecule to the other. More rapid spatial oscillations imply the existence of higher-energy components in the intermolecular region and can therefore be neglected there altogether. *Within* a molecule, the spatial oscillations lowest in energy can be represented by atomic orbitals, the most important being 1s, 2s, 3s..., etc. To first order, these have the same leading form, i.e., $e^{(-r/a_0)}$.

*Work supported in part by NASA (Grant No. NGR-33-010-188) and NSF through the facilities of the Materials Science Center (Grant No. DMR-72-03029).

† Present address: Instituto de Física, Universidad Católica de Chile, San Joaquín, Santiago, Chile.

¹R. Monnier, E. L. Pollock, and C. Friedli, *J. Phys. C* **7**, 2467 (1974); for more details and additional considerations, see R. Monnier, thesis (Université de Neuchâtel, Switzerland, 1974) (unpublished).

²C. Friedli, Ph.D. thesis (Cornell University, 1975) (unpublished).

³F. S. Ham and B. Segall, *Phys. Rev.* **124**, 1786 (1961).

⁴F. S. Ham and B. Segall, *Methods in Computational Physics: Energy Bands in Solids* (Academic, New York, 1968), Vol. 8, p. 251.

⁵T. Loucks, *Augmented Plane Wave Method* (Benjamin, New York, 1967).

⁶G. S. Painter, *Phys. Rev. B* **7**, 3520 (1973).

⁷See, for example, G. S. Painter and D. E. Ellis, *Phys. Rev. B* **12**, 474 (1970).

⁸G. Pastori Parravicini, I. Villa, and M. Vittori, *Phys. Status Solidi B* **67**, 345 (1975).

⁹D. E. Ramaker, L. Kumar, and F. E. Harris, *Phys. Rev. Lett.* **34**, 812 (1975).

¹⁰E. Brown and J. A. Krumhansl, *Phys. Rev.* **109**, 30 (1958).

¹¹H. M. James and J. C. Raich, *Phys. Rev.* **162**, (1967).

¹²H. M. James, *Phys. Rev. B* **2**, 2213 (1970).

¹³R. J. Lee and J. C. Raich, *Phys. Rev. B* **5**, 1591 (1972).

¹⁴H. Meyer, F. Weinhaus, B. Marariglia, and R. L. Mills, *Phys. Rev. B* **6**, 1112 (1972).

¹⁵C. J. Bradley and A. P. Cracknell, *The Mathematical Theory of Symmetry in Solids* (Clarendon, Oxford, 1972), pp. 133, 377, and 416; see also, T. A. Scott,

Phys. Rep. 27, 99 (1976).

¹⁶In principle, the minimum region in the zone that must be considered is the *representation domain* and not the smaller *basic domain*. As defined by Bradley and Cracknell (Ref. 15), the former generates regions which will cover the Brillouin zone exactly under the action of all the operations of the point group to which the space group of the structure is isogonal. (It is obtained by taking all the point-group operations present from among the operations of that space group.) The basic domain is defined in the same way except that the isogonal point group is replaced by the full holosymmetric point group of the crystal system to which the structure belongs. In the present case it is the cubic system. This distinction is necessary (as is this footnote) because of the curiosity that of the 230 space groups *Pa3* alone is anomalous and there are differences in the irreducible representations along certain ostensibly *equivalent* directions in the zone: correspondingly, there should be differences in the

energy eigenvalues for electrons (or phonons) for such directions. In fact, this was indeed found to be the case for the bands of *Pa3* molecular hydrogen, but the calculated differences in energy along such directions (along Z^1 and Z^{15}) are sufficiently small that for our purposes, where high densities are of primary concern, only the usual basic domain needs to be considered.

¹⁷G. Baldini, Jpn. J. Appl. Phys. Suppl. 14, 613 (1965).

¹⁸L. Schmidt, Phys. Lett. A 36, 87 (1971).

¹⁹See A. Gedanken, B. Raz, and J. Jortner, J. Chem. Phys. 59, 2752 (1973); and Ref. 8.

²⁰A. Zunger, J. Phys. Chem. Solids, 36, 229 (1975).

²¹A. K. McMahan, B. L. Hoard, and M. Ross, Phys. Rev. B 15, 726 (1977).

²²D. Straus and N. W. Ashcroft, Phys. Rev. Lett. 38, 415 (1977).

²³D. Straus, thesis (Cornell University, 1977) (unpublished) (Materials Science Center Report No. 2739).

²⁴J. C. Slater, *Quantum Theory of Molecules and Solids* (McGraw Hill, New York, 1963), Vol. 1, pp. 23–25.